University of Massachusetts Medical School

eScholarship@UMMS

2021-02-15

Quantifying and Mitigating Motor Phenotypes Induced by Antisense Oligonucleotides in the Central Nervous System [preprint]

Michael P. Moazami
University of Massachusetts Medical School

Et al.

Let us know how access to this document benefits you.

Follow this and additional works at: https://escholarship.umassmed.edu/faculty_pubs

Part of the Biochemistry Commons, Medicinal Chemistry and Pharmaceutics Commons, Molecular and Cellular Neuroscience Commons, Nervous System Commons, Nervous System Diseases Commons, Neurology Commons, Nucleic Acids, Nucleotides, and Nucleosides Commons, Pharmacology Commons, and the Toxicology Commons

1   **Quantifying and Mitigating Motor Phenotypes Induced by Antisense Oligonucleotides in the Central**

2   **Nervous System**

3   Michael P. Moazami,[1, ‡] Julia M. Rembetsy-Brown,[1,‡] Feng Wang,[1] Pranathi Meda Krishnamurthy,[1]

4   Alexandra Weiss,[2] Miklos Marosfoi,[3] Robert M. King,[3,4] Mona Motwani,[5] Heather Gray-Edwards,[3]

5   Katherine A. Fitzgerald,[5] Robert H. Brown,[2] Jonathan K. Watts[1,6] *

6   [1]RNA Therapeutics Institute, University of Massachusetts Medical School, Worcester, MA, 01605 USA;

7   [2]Department of Neurology, University of Massachusetts Medical School, Worcester, MA, 01605 USA;

8   [3]Department of Radiology, UMass Medical School, Worcester, MA, 01605 USA; [4]Department of

9   Biomedical Engineering, Worcester Polytechnic Institute, Worcester, MA, 01609, USA; [5]Program in

10 Innate Immunity, Division of Infectious Diseases and Immunology, Department of Medicine, University

11 of Massachusetts Medical School, Worcester, MA, 01605 USA; [6]Department of Biochemistry and

12 Molecular Pharmacology, University of Massachusetts Medical School, Worcester, MA, 01605 USA

13 *To whom correspondence should be addressed:

14 Phone, 774-455-3784; Email, jonathan.watts@umassmed.edu

15 ‡These authors contributed equally to the work

16

17 **ABSTRACT**

18 Antisense oligonucleotides (ASOs) are emerging as a promising class of therapeutics for neurological

19 diseases. When injected directly into the cerebrospinal fluid, ASOs distribute broadly across brain

20 regions and exert long-lasting therapeutic effects. However, many phosphorothioate (PS)-modified

21 gapmer ASOs show transient motor phenotypes when injected into the cerebrospinal fluid, ranging from

22 reduced motor activity to ataxia or acute seizure-like phenotypes. The effect of sugar and phosphate

23 modifications on these phenotypes has not previously been systematically studied. Using a behavioral

24 scoring assay customized to reflect the timing and nature of these effects, we show that both sugar and

25 phosphate modifications influence acute motor phenotypes. Among sugar analogues, PS-DNA induces

26 the strongest motor phenotype while 2'-substituted RNA modifications improve the tolerability of PS-

27 ASOs. This helps explain why gapmer ASOs have been more challenging to develop clinically relative to

28 steric blocker ASOs, which have a reduced tendency to induce these effects. Reducing the PS content of

29 gapmer ASOs, which contain a stretch of PS-DNA, improves their toxicity profile, but in some cases also

30 reduces their efficacy or duration of effect. Reducing PS content improved the acute tolerability of ASOs

31 in both mice and sheep. We show that this acute toxicity is not mediated by the major nucleic acid

32   sensing innate immune pathways. Formulating ASOs with calcium ions before injecting into the CNS

33   further improved their tolerability, but through a mechanism at least partially distinct from the

34   reduction of PS content. Overall, our work identifies and quantifies an understudied aspect of

35   oligonucleotide toxicology in the CNS, explores its mechanism, and presents platform-level medicinal

36   chemistry approaches that improve tolerability of this class of compounds.

37

38   **INTRODUCTION**

39   Antisense oligonucleotides (ASOs) are emerging as a promising class of therapeutics for neurological

40   diseases.[1-4]   The groundbreaking ASO nusinersen was approved by the FDA in 2016 to treat spinal

41   muscular atrophy.[5-12] Nusinersen operates through a splice-switching mechanism and is fully modified

42   with 2'-O-methoxyethyl sugars and phosphorothioate linkages. Nusinersen showed an excellent safety

43   and efficacy profile in clinical trials. Another class of ASOs is designed to recruit RNase H to cleave target

44   RNA and thus silence gene expression. These so-called gapmer ASOs require a stretch ("gap") of 8-10

45   non-sugar-modified DNA nucleotides in the middle to enable RNase H recruitment. In contrast to

46   nusinersen, early clinical evaluation of gapmer ASOs in the CNS faced dose-limiting toxicity resulting in

47   failed clinical trials. Nevertheless, after these false starts, a more advanced generation of gapmer ASOs

48   are in clinical development for neurological diseases including Huntington's disease,[13-15] Alzheimer's

49   disease,[16] Parkinson's disease,[17] and amyotrophic lateral sclerosis (ALS).[4, 18-20] These compounds show

50   promising biomarker efficacy with reasonable toxicity profiles.

51   Looking at the chemical modification patterns used in early clinical trials vs RNase H-active compounds

52   currently in the clinic, a major difference is the number of PS backbone modifications. In early trials,

53   gapmer ASOs were fully PS modified (similar to nusinersen), while current variants of the compounds

54   use a mixed backbone where up to six linkages are substituted back to phosphodiester. In parallel in our

55   own work, during the development of gapmer ASOs for *C9ORF72*-driven ALS,[21] we observed a range of

56   transient motor phenotypes most severe within the first 1-3 hours after intracerebroventricular

57   administration of the ASOs to mice. We were able to reduce these effects by reducing the backbone PS

58   content. We carried out the current study to explore the generality of this phenomenon, explore its

59   mechanism, and understand how it is affected by chemical modifications to both phosphates and

60   sugars.

61   Using a quantitative scoring assay for ASO-induced motor phenotypes, we now show that the acute

62   motor phenotypes produced by PS-modified gapmer ASOs in the brain can be minimized by using ASOs

63   containing a combination of phosphorothioate (PS) and unmodified phosphodiester (PO) linkages.

64   Interestingly, the ASO-induced motor phenotypes are profoundly affected by the sugar modifications

65   used: PS-DNA ASOs were the most toxic, while ASOs composed entirely of 2'-O-substituted RNA (2'-O-

66   methoxyethyl or 2'-O-methyl RNA) were less toxic.

67   We also now present experimental results that shed light on the mechanism underlying the observed

68   motor phenotypes. We show that they are not mediated by the major nucleic acid sensing innate

69   immune pathways, do not produce long-term toxicity and are observed in both small (mouse) and large

70   (sheep) brains. The toxicity profile of *both* fully PS and mixed-backbone (PO/PS) ASOs can be improved

71   by exposing ASOs to calcium-containing buffers before injection, indicating that PS-modified

72   oligonucleotides induce a local CSF disbalance in divalent ion composition. Finally, we show that mixed

73   (PO/PS) backbone ASOs with *in vivo* gene silencing efficacy comparable with full PS ASOs can be

74   engineered, defining the clear steps towards development of highly active and safe ASOs for other

75   neurodegenerative disorders.

76   Progress in chemical modification of oligonucleotides has been profoundly important in enabling clinical

77   success.[22-24] Further improvements in modification and formulation of ASOs, as well as increased

78   mechanistic understanding of the factors defining efficacy and toxicity, is essential to expand the

79   therapeutic use of gapmer ASOs in the CNS.

80   **RESULTS**

81   **EvADINT scoring assay for acute behavioral toxicity**

82   After administration of ASOs into the CNS, we observed dose-dependent acute behavioral toxicity that

83   varied from lethargy, lack of responsiveness and ataxia to hyperactivity, seizures, and, in extreme cases,

84   death. This behavioral neurotoxicity was most striking in the first 1-3 hours after administration. Even

85   severely affected mice, unless they died, recovered fully by 24h and showed no further adverse effects.

86   To describe our studies of acute toxicity in a robust way, we needed a way to quantify this acute toxicity.

87   Various protocols have been used to quantitate behavioral toxicity under the umbrella of a "Functional

88   Observational Battery" (FOB), with variations for both acute and longitudinal neurotoxicity (reviewed in

89   ref [25]. Regulatory documents such as the OECD guideline for neurotoxicity testing in rodents[26] do not

90   provide assay details that are well aligned with the transient toxicity seen after ASO administration to

91   mice.

92   We therefore developed a scoring assay optimized to quantify the transient motor phenotypes induced

93   after intracerebral oligonucleotide injection. We call this assay EvADINT (Evaluation of Acute Drug-

94   Induced NeuroToxicity). In this assay, we monitored mice at multiple time points over 24 hours after

95   injection, assigning a score for various parameters as described in Table 1. If a mouse died, it was given a

96   score of 75. Seizures, hyperactivity and other atypical motor behavior were scored depending on their

97   severity. The rest of the score was allotted based on how much time elapsed before the animal was able

98   to resume various aspects of normal mouse behavior. We weighted the observed phenotypes according

99   to their apparent severity. For example, sternal posture was weighted more heavily than normal

100   grooming since mice must be able to right themselves to carry out most other aspects of normal mouse

101   behavior, and because maintenance of sternal posture is simpler than eating, walking or grooming. For

102   similar intuitive reasons, seizures and death were weighted more heavily than the other factors such as

103   latency to resume normal mouse behavior(s). We varied the relative weightings of different factors in

104   our assay – death, seizures, and the various other behavioral observations – and observed that the

105   relative scores of different ASOs were very similar in all cases. Thus, the EvADINT scoring assay is robust

106   to variation in the precise weights assigned to each factor.

Behavioral element / observation					
Death	**75**				
	Severe	Moderate		Mild	Absent
Seizure[a]	20	15		10	0
Hyperactivity or other atypical motor behavior[b]	15	10		5	0
Time required for:	0.5 h	1 h	2 h	4 h	≥24 h
Maintenance of sternal posture	0	4	8	12	20
Unstimulated movement	0	3	6	9	15
Movement without ataxia	0	2	4	6	10
Normal grooming/eating/nesting	0	1	2	3	5

107

108   **Table 1.** Breakdown of scoring for the EvADINT system for quantification of acute motor phenotypes. Examples of observed

109   phenotypes (movies and corresponding scores), and all actual mouse scores for all figures are given in the supporting

110   information. Personnel were blinded to ASO group during the scoring. [a]Severity of seizures was ranked as follows: A *severe*

111   seizure had a duration of >30min and/or with constant or high intensity muscle contractions. A *moderate* seizure had a 10-30

112   min duration and moderate intensity muscle contractions or rapid and repetitive synchronous twitching, accompanied by

113   apparent short-term loss of consciousness. A *mild* seizure lasted <10min and featured low intensity muscle contractions or

114   short & infrequent bursts. [b]Severity of hyperactivity or other atypical motor behavior was ranked as follows. Severe: >30min

4

115   duration, popcorning/jumping, constant. Moderate: 10-30min duration, slight hopping, other atypical motor behavior. Mild:
116   <10min duration, uncoordinated movements, twitching.

117

Reduced phosphorothioate content and formulation with Ca^{2+} reduces acute toxicity

119   In our parallel work on the development of ASOs that target the sense and antisense transcripts from

120   the ALS/FTD gene *C9ORF72*, we found that reducing the number of phosphorothioate-modified linkages

121   between pairs of 2'-*O*-methoxyethyl (MOE)-modified ribonucleotides improved tolerability without loss

122   of efficacy or duration of effect.[21] A similar mixed backbone design is now in clinical development.[15]

123   Thus our lead backbone design, and the mixed backbone design that we focus on exclusively in this

124   study, contains a single PS linkage at each end of the ASO, followed by three PO linkages and then PS

125   linkages throughout the remaining (central) portion of the ASO (sequences and modification patterns

126   are shown in Table 2). With the EvADINT scoring system established, we set out to quantify this

127   observation and explore its generality and mechanism. We first established that our previous result was

128   reproducible under quantitative, blinded conditions. Thus, reducing the phosphorothioate content of a

129   *C9ORF72*-targeted ASO led to increased tolerability in the CNS (Figure 1A).

130   Phosphorothioate groups are more acidic than phosphates, and thus more anionic at physiological pH,

131   and a greater share of the negative charge is concentrated on the sulfur atom. We wondered whether

132   the more anionic character of phosphorothioate-modified ASOs was increasing their tendency to chelate

133   divalent cations from CSF. During ICV injections, to keep volumes small, the ASO concentration is high

134   (typically 1-4 mM). This is comparable to or higher than the concentration of Ca^{2+} in CSF, which is 1.3–

135   1.4 mM[27] – and moreover, each polyanionic ASO could potentially chelate multiple Ca^{2+} ions. We

136   wondered whether reducing the PS content of our ASOs was reducing toxicity simply by reducing their

137   tendency to chelate Ca^{2+} ions.

138   To explore whether the neurotoxicity we observed could be explained by Ca^{2+} chelation, we tested ASOs

139   that had been pre-saturated with Ca^{2+} before injection. We chose this pre-saturation approach because

140   we did not know exactly how much Ca^{2+} each ASO would chelate from the solution. We were concerned

141   that if we simply suspended our ASOs in buffer containing a physiological concentration of Ca^{2+}, it might

142   be insufficient to compensate for the chelation abilities of ASOs at these high concentrations. And on

143   the other hand, we were concerned that injecting ASOs in buffer containing higher-than-physiological

144   concentrations of Ca^{2+} might lead to hypercalcemia-mediated toxicity. Thus, after HPLC purification of

145   ASOs, we transferred each ASO to a 3kDa-cutoff Amicon ultrafiltration cartridge, and washed with a

146   solution containing 20 mM Ca^{2+}, twice with water, and once with PBS.[28] We then resuspended the ASO

147   in PBS and proceeded to injection. The intervening water washes are important to prevent the

148   irreversible precipitation of calcium phosphate resulting from excess Ca^{2+} in the presence of phosphate
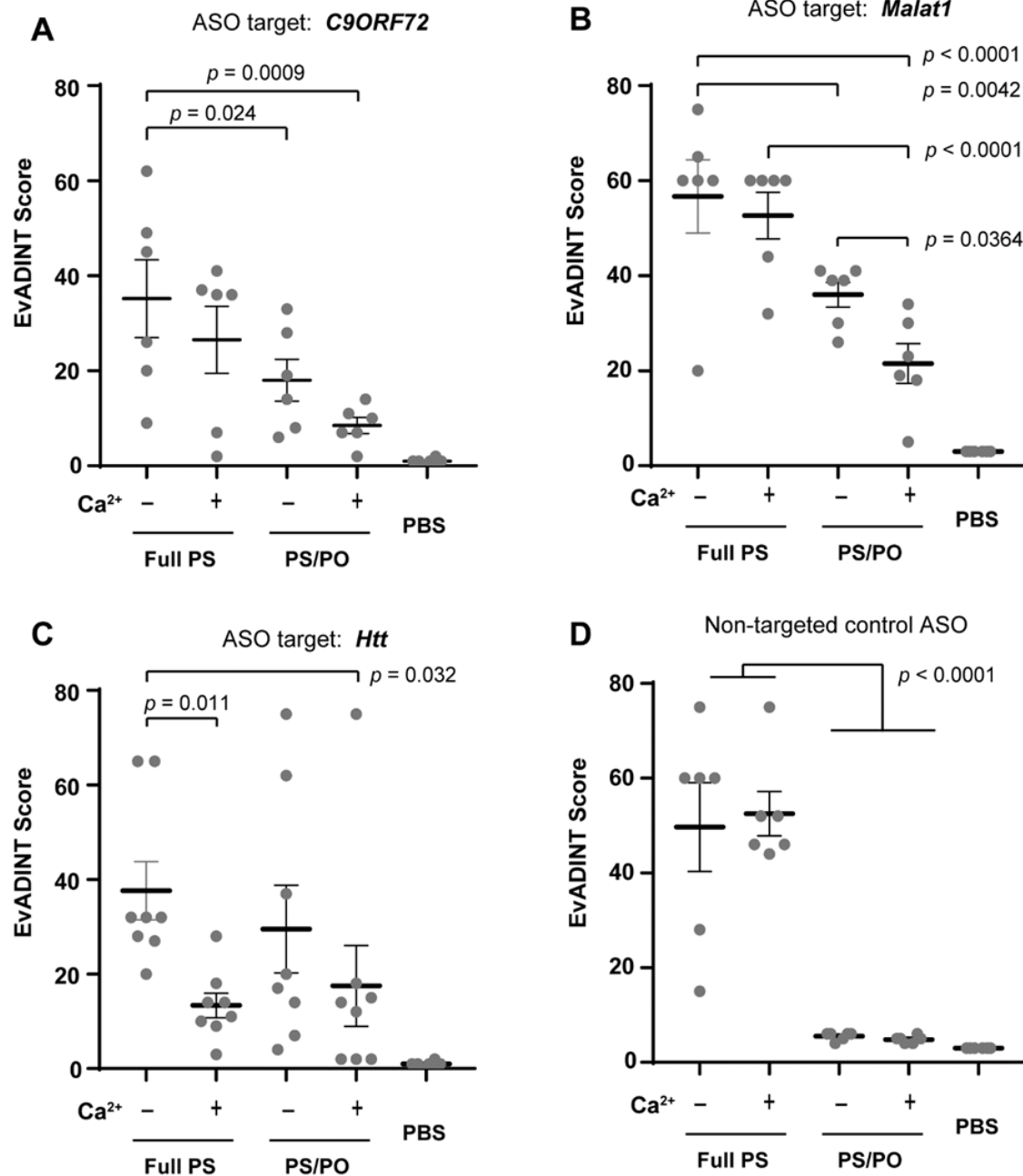
149   buffer.

150   For this study, we chose a moderately high dose of 35 nmol ASO per mouse (equivalent to about

151   10mg/kg), somewhat higher than the dose typically required for effective gene silencing. Under these

152   conditions, for our *C9ORF72*-targeted ASO, we observed that pre-saturation with Ca^{2+} led to a robust

153   improvement in acute tolerability in the CNS (Figure 1A). Interestingly, the improvement in tolerability

154   occurred for both the full PS and the mixed backbone ASOs. Thus, the best-tolerated ASO was the

155   compound with reduced PS content and which had also been pre-saturated with Ca^{2+}.

156   These C9ORF72 ASOs targeted the human transcript; the acute motor phenotypes were observed

157   whether the ASOs had a target (as in the transgenic C9ORF72 mouse models we used in the parallel

158   work on therapeutic development for C9ORF72)[21] or not (as in the wild type mice used here).

159   To test whether these principles applied to other targeting and non-targeting sequences, we synthesized

160   ASOs targeting the noncoding RNA *Malat1* and the Huntingtin (*Htt*) mRNA (Sequences **6**–**9**, Table 2). We

161   synthesized versions of these sequences in both full PS and mixed backbone formats, and in all cases

162   compared simple formulation in PBS with formulation in PBS after calcium pre-saturation. We injected

163   these compounds into mice (ICV) and observed motor phenotypes using the EvADINT assay (Figure 1B-

164   C). For the *Malat1*-targeting ASO (Figure 1B), we saw the same pattern as for the *C9ORF72*-targeted

165   ASO – namely, there was a substantial improvement in tolerability upon reducing the PS content, and

166   both the full PS and mixed backbone ASOs showed further improvement upon formulation with Ca^{2+}.

167   For the *Htt*-targeted ASO, we saw higher toxicity and broader variability in tolerability across the groups

168   (Figure 1C). The improvement in tolerability of this mixed-backbone design was less clear than for the

169   other sequences. However, the improvement in tolerability from Ca^{2+} formulation was robust in the

170   context of both backbone variants. Thus, there may be a sequence-dependence to optimal backbone

171   design, and it is clear that reducing the PS content in this way does not reduce the need to select good

172   sequences.

173   Finally, we synthesized non-targeting control ASOs (Sequences **10** and **11**, Table 2) and formulated them

174   in the same way as the first three sequences. We injected these ASOs into mice and scored neurotoxicity

6

175   using the EvADINT assay (Figure 1D). The patterns observed for this sequence are slightly different – in

176   this case, calcium formulation had little or no effect on toxicity, while the reduction of PS content

177   showed a dramatic improvement in toxicity.

178   Thus, each of the four sequences we tested showed a robust improvement in toxicity following a

179   modest reduction in PS content, Ca^{2+} formulation, or both. The ASO-induced motor phenotypes were

180   dose dependent across multiple sequences and design patterns (Supporting Figure S1). It is interesting

181   that across all sequences, higher toxicity was often accompanied with higher inter-animal variability.

182   That is, there appear to be important animal-to-animal variations in the actualization of this toxicity.

183

184

Seq #	Name	Sequence and modification pattern	Mass calculated	Mass observed
1	C9ORF72-full PS	GsCsCsCsCsTsAsGsCsGsCsGsCsGsAsCsTsC	6560.6	6560.0
2	C9ORF72-PS/PO	GsCoCoCoCsTsAsGsCsGsCsGsCsGoAoCoTsC	6465.6	6465.2
3	C9ORF72-DNA+PS	GsCsCsCsCsTsAsGsCsGsCsGsCsGsAsCsTsC	5820.8	5820.6
4	C9ORF72-MOE+PS	GsCsCsCsCsTsAsGsCsGsCsGsCsGsAsCsTsC	7153.3	7154.3
5	C9ORF72-OMe+PS	GsCsCsCsCsTsAsGsCsGsCsGsCsGsAsCsTsC	6332.0	6332.8
6	MALAT1-full PS	GsGsGsTsCsAsGsCsTsGsCsCsAsAsTsGsCsTsAsG	7232.1	7231.9
7	MALAT1-PS/PO	GsGoGoToCsAsGsCsTsGsCsCsAsAsTsGoCoToAsG	7136.3	7135.2
8	HTT-full PS	CsTsCsGsAsCsTsAsAsAsGsCsAsGsGsAsTsTsTsC	7217.1	7216.8
9	HTT-PS/PO	CsToCoGoAsCsTsAsAsAsGsCsAsGsGsGsAoToToTsC	7120.7	7120.0
10	NTC-full PS	CsCsTsAsTsAsGsGsAsCsTsAsTsCsCsAsGsGsAsA	7184.1	7184.0
11	NTC-PS/PO	CsCoToAoTsAsGsGsAsCsTsAsTsCsCsAoGoGoAsA	7088.1	7087.1

185 **Table 2.** Sequences used in this study. Bold blue: MOE. Bold green: 2'-OMe. Black: DNA. Lower case

186 letters s and o refer to phosphorothioate and phosphodiester linkages, respectively. NTC: non-target

187 control ASO.

188

Figure 1. The tolerability of ASOs administered into the CNS is improved by modestly reducing the backbone PS content and by formulating with Ca^{2+} ions before injecting. Mice were injected ICV with 35 nmol of each ASO in 10 μL PBS (or with 10 μL PBS as control) and behavior was scored by a blinded investigator over the following 24h using the EvADINT rubric. Sequences targeting (A) *C9ORF72*, (B) *Malat1*, or (C) *Htt*, or (D) a non-targeting control ASO, showed improvements in acute tolerability upon reducing the PS content, formulating with Ca^{2+} ions, or both. Each data point represents the EvADINT score from one mouse; n = 6–8; error bars represent SEM. P-values are calculated using one-way ANOVA within GraphPad Prism software and represent per-comparison error rates. Full sequences and modification patterns are given in Table 2.

199 **Sugar 2'-modifications reduce acute motor phenotypes**

200 Nusinersen, approved to treat spinal muscular atrophy,[9-12] contains a fully phosphorothioate backbone.

201 Yet it is well tolerated in the CNS[8] and has received FDA approval.[5, 6] This compound is modified at each

202 nucleotide with MOE; it is not a gapmer and does not require a stretch of DNA because it functions to

203 redirect splicing rather than recruiting RNase H. We therefore wondered whether fully-

204 phosphorothioate-modified ASOs containing different sugar modifications might show acute motor

205 phenotypes to a different extent.

206 To study this question, we synthesized fully-phosphorothioate ASOs modified *at every nucleotide* with

207 DNA, 2'-O-methyl RNA, or MOE, respectively (in contrast to the gapmer designs used in Figure 1). We

208 suspended these in PBS, injected them ICV at 35 nmol/mouse and scored acute motor phenotypes using

209 the EvADINT assay. The fully DNA oligonucleotide **3** was dramatically more toxic than the two

210 oligonucleotides containing 2'-modifications at every nucleotide (**4** and **5**; Figure 2). The two 2'-modified

211 versions showed a dramatic reduction in motor phenotypes. We also carried out the comparison of full

212 MOE with full DNA for a sequence targeting Malat1 and saw the same dramatic difference in toxicity

213 (data not shown: the Malat1 experiment was carried out before we had established the quantitative

214 EvADINT assay, but the clear difference we observed strongly suggests that the impact of sugar

215 modification on toxicity is not sequence specific.)

216
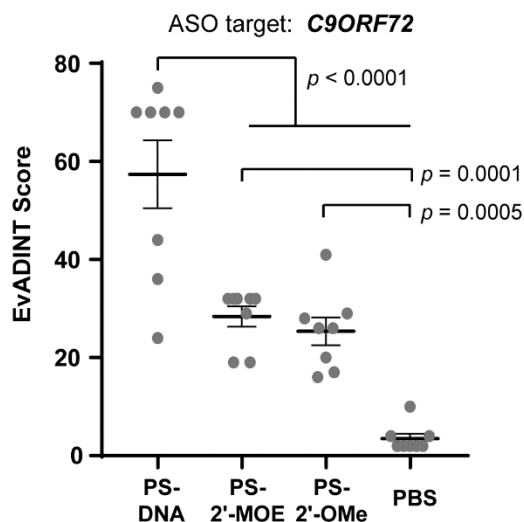
217

218 **Figure 2.** Fully PS ASOs containing 2'-modifications at each position are less toxic than those containing DNA at

219 each position. We injected 35 nmol of each ASO in PBS to the right lateral ventricle of mice, and recorded

220 behavioral outcomes according to the EvADINT rubric. Each data point represents the EvADINT score from one

221   mouse; n = 8; error bars represent SEM. P-values are calculated using one-way ANOVA within GraphPad Prism

222   software and represent per-comparison error rates. Full sequences and modification patterns are given in Table 2.

223

PS-ASO-induced acute neurotoxicity is not mediated by the major nucleic acid sensing innate immune

pathways

226   The acute toxicity we observe is most intense in the first hour after injection of mice. This timing

227   suggested to us that the acute toxicity is not mediated by the innate immune system, since innate

228   immune responses to nucleic acid stimuli typically do not peak until several hours after stimulation.[29, 30]

229   To confirm in a more direct way whether innate immune responses could play a role, we directly

230   evaluated whether there was any contribution to this neurotoxicity from signaling through Toll-like

231   receptors (TLRs) 3, 7, or 9, or the CGAS-STING pathway. First, we evaluated mouse behavior after

232   injecting a 50 μg dose of poly(I:C), a compound and dose known to induce potent innate immune

233   stimulation through TLR3 or MDA-5.[29,31] Mice treated with poly(I:C) showed no evidence of the acute

234   motor phenotypes seen with PS-modified ASOs, with EvADINT scores comparable to the buffer-only

235   control mice (Figure 3A).

236   We also evaluated the role of other endosomal receptors TLRs 7 and 9 as well as the cytosolic DNA

237   sensing cGAS-STING pathway by obtaining mice lacking both MyD88 and STING (Myd88$^{-/-}$ STING$^{-/-}$ double

238   knockout mouse). This strain lacks signaling components for both endosomal as well as cytosolic nucleic

239   acid sensing pathways. TLRs 7 and 9 signal through MyD88, whereas STING functions downstream of

240   cGAS following cytosolic DNA sensing. Injection of a PS-DNA ASO into these double knockout mice

241   showed an identical response relative to a background-matched control mouse, confirming that the

242   toxicity is not mediated by any of these nucleic acid sensors (Figure 3B).

243   Taken together, these experiments provide evidence that the acute toxicity which is the focus of this

244   work is not mediated by the major nucleic acid sensing innate immune pathways. Of course, this finding

245   does not preclude a role for other oligonucleotide-induced innate immune responses in the brain at

246   longer timepoints, as described by other authors.[32]

247

248
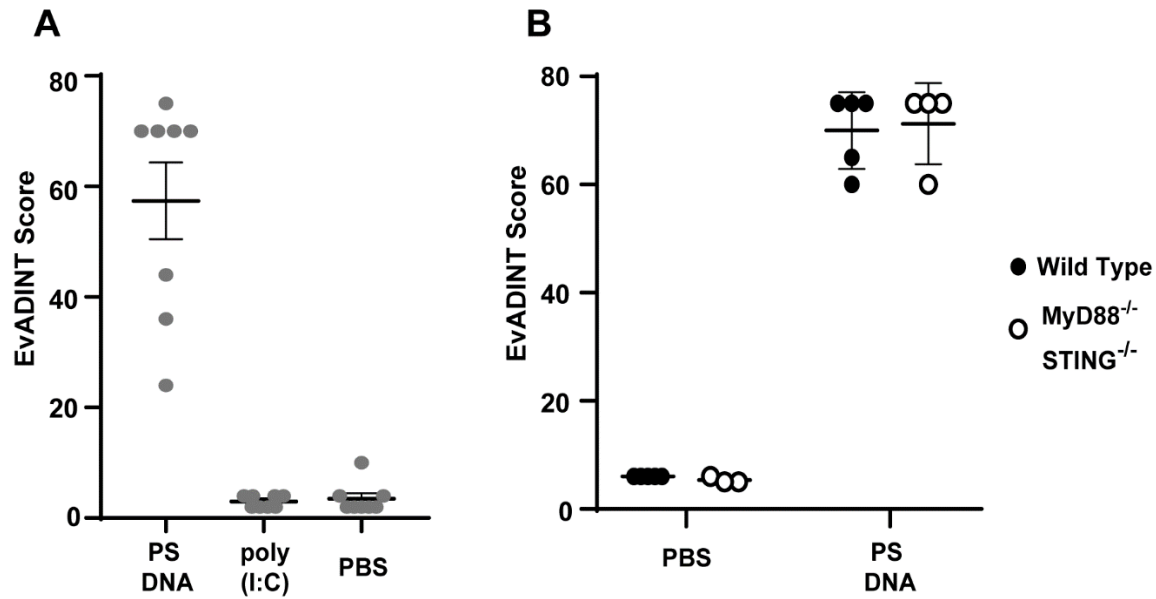
Figure 3. The acute neurotoxicity we observe is not mediated by toll-like receptors 3, 7, or 9, by MDA-5, or by the cGAS-STING pathway. (A) The highly immunogenic compound poly(I:C) produces none of the behavioral toxicity seen for the PS-containing ASOs after ICV injection, showing that the toxicity is not signaling through TLR3 or MDA-5. We injected 35 nmol of PS-DNA or 50 µg of poly(I:C) in PBS to the right lateral ventricle of mice, and recorded behavioral outcomes according to the EvADINT rubric. (B) Double knockout MyD88^{-/-} STING^{-/-} mice (hollow dots) show an identical response to wild type mice (filled dots), showing that the acute toxicity is not mediated by TLR7, TLR9 or the CGAS-STING pathway. In both panels, each data point represents the EvADINT score from one mouse; error bars represent SEM. All PS-DNA samples were significantly different from all other samples in both panels (One-way ANOVA, $p < 0.0001$). Full sequences and modification patterns are given in Table 2.

258

259

260 **The improved tolerability of mixed backbone ASOs applies to large brains**

261 We wondered whether the acute toxicity we observed was an artifact of the small brain size of mice.

262 This would make the concern significantly less relevant to researchers interested in therapeutic

263 development of ASOs. To test whether the phenomenon applied to larger brains, we injected two

264 sheep with fully phosphorothioate ASO (C9ORF72-full PS, Sequence **1**), and four sheep with the mixed

265 backbone analogue of the same sequence (C9ORF72-PS/PO, Sequence **2**).

266 Direct intrathecal injection, the route used for patients receiving ASO therapeutics, is not practical in

267 sheep because of difficulty accessing the intrathecal compartment and because CSF tends to be expelled

268 from the site where the dura is punctured, leading to poor uptake of ASO. Therefore, we used a

269 technique whereby a microcatheter was threaded up though the intrathecal space and the ASO was

270 delivered directly into the cisterna magna (see Methods). In all cases successful microcatheter

271 navigation was performed into cisterna magna. Both intracisternal contrast injection and cone beam

272 computed tomography confirmed the correct catheter position prior to ASO injection. Contrast material

273 opacification was seen in the cisterna magna, around the cerebellum and in the upper cervical spinal

274 canal. No complication was observed in relation to catheter navigation or contrast injection.

275 None of the four sheep that were given the mixed backbone ASO (C9ORF72-PS/PO, Sequence **2**) showed

276 evidence of abnormal motor phenotypes. In contrast, both sheep that were given fully

277 phosphorothioate ASO (C9ORF72-full PS, Sequence **1**) showed hindlimb weakness and gait instability

278 (wobbliness) within the first 24 hours. Thus, the acute toxicity of fully phosphorothioate ASOs is not

279 specific to mice but also applies to large brains. The ASOs were given in Lactated Ringer's solution, a

280 calcium-containing diluent readily available at USP-grade, which confirms that the toxicity improvement

281 mediated by reducing PS content is at least partly distinct from the question of Ca^{2+} chelation, in larger

282 brains (in this case, sheep) as in mice as described above.

283

284 **Impact on efficacy of reducing phosphorothioate content and Ca^{2+} formulation**

285 We previously observed for *C9ORF72*-targeted ASOs that the mixed backbone strategy did not reduce

286 potency or efficacy as long as the phosphodiester linkages were between MOE nucleotides on both

287 sides. In contrast, when we modified the linkage between a MOE nucleotide and a deoxynucleotide, the

288 potency dropped dramatically.[21] Thus, in this paper we have focused on a single mixed backbone

12

289   design, in which the three internal linkages in each MOE wing were PO, and all other positions were PS.

290   To study the effect on efficacy of this backbone design across these sequences, we compared the gene

291   silencing of ASOs against HTT and MALAT1 in their full PS and mixed backbone versions. To be able to

292   discriminate between compound efficacy, we chose a non-saturating dose for this element of our study:

293   we therefore injected 15 nmol of each ASO ICV, and harvested brains after 3 weeks.

294   We found that both HTT and MALAT1-targeted ASOs significantly reduced their target mRNA expression,

295   but there was a trend to reduced efficacy in mixed backbone format relative to the fully PS analogues

296   (Figure 4A-B). It is not clear whether this results from a reduction in nuclease stability or a reduction in

297   cellular uptake, since the PS linkage contributes to both factors. Nevertheless, this finding suggests that

298   there is merit in exploring alternate backbone architectures, including next-generation mixed backbone

299   designs,[33] that might allow improvements in acute toxicity while maintaining or improving potency and

300   efficacy.

301   Next, we tested whether calcium pre-saturation affected ASO efficacy. We prepared ASOs by dissolving

302   in PBS, either with or without a Ca^{2+} pre-saturation step, and injected them ICV into mice. In the context

303   of either a full PS or mixed PO/PS backbone, we observed that gene silencing efficacy was not affected

304   by the presence of the Ca^{2+} pre-saturation step (Figure 4C).
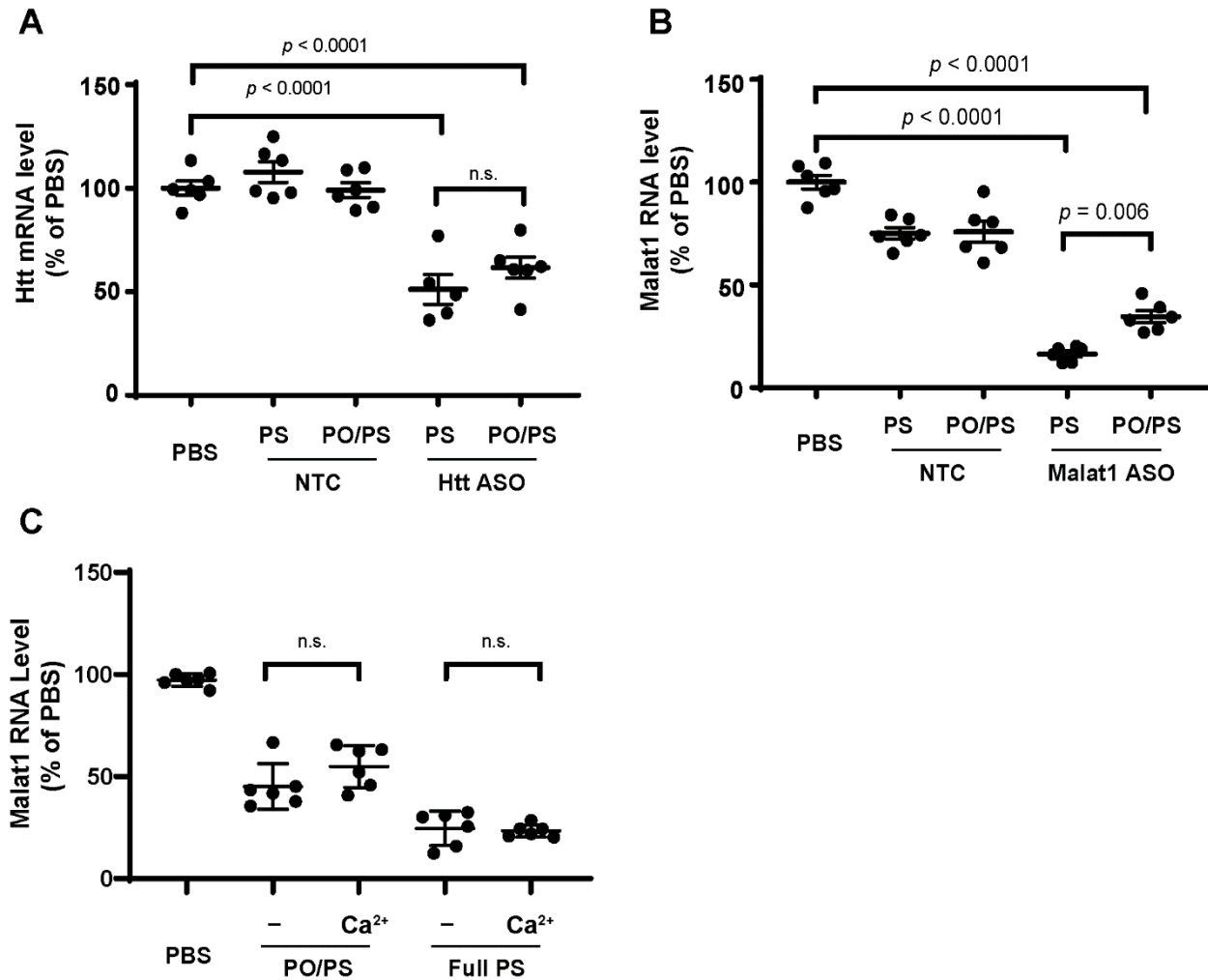
Figure 4. Effect of phosphorothioate reduction and calcium formulation on ASO efficacy. (A,B) Silencing of (A) *Htt* and (B) *Malat1* RNA three weeks after a 15 nmol dose of either full PS of mixed backbone (PO/PS) ASOs. Each data point represents one mouse; n=6 mice. (C) Formulation with calcium does not affect the gene silencing efficacy of ASOs. ASOs were resuspended and delivered in PBS, with or without first saturating the ASOs with calcium (see methods). In all panels, statistical significance was evaluated by one-way ANOVA followed by Tukey's multiple comparisons test. Sequence numbers relate to the sequences and modification patterns given in Table 2.

14

313   **DISCUSSION**

314   Over the past few years, an increasing number of papers have described the use of gapmer ASOs in the

315   CNS. Many of these studies employ ASOs containing full-PS backbones[4, 13, 34-36] or those for which the

316   modification pattern is not clearly disclosed.[16, 18, 37, 38] Other recent papers do describe ASOs containing

317   a mixture of PS and PO linkages for use in the CNS.[15, 17, 19, 20, 36, 39-42] However, to the best of our

318   knowledge, no comparative data on the neurotoxicology of these mixed-backbone ASOs relative to fully-

319   PS ASOs has been presented, nor has the relationship of sugar modification with acute motor

320   phenotypes been previously known or the underlying mechanism explored before now.

321   The mechanism for the acute neurotoxicity of PS-modified ASOs is likely multifactorial. We initially

322   wondered whether the more polyanionic nature of PS linkages was increasing chelation of divalent ions

323   by ASOs. Since divalent cations, and Ca^{2+} in particular, are key for synaptic signaling and

324   neurotransmission,[43, 44] such depletion of divalent cations from CSF would be expected to produce acute

325   toxicity that would be expected to last until homeostasis of Ca^{2+} concentration in CSF was restored. Ca^{2+}

326   chelation has been responsible for unexpected toxicities in other classes of drugs.[45] Supporting a role

327   for this mechanism, pre-saturating ASOs with Ca^{2+} before injection improved their tolerability. Other

328   groups have observed ASO-mediated Ca^{2+} chelation in cultured neurons.[46] However, mixed backbone

329   strategies improved toxicity even in the presence of such divalent ions, which suggests that Ca^{2+}

330   chelation cannot fully explain the acute motor phentoypes induced by PS-modified gapmer ASOs.

331   Our experiments document that ASO-induced transient motor phenotypes are not a downstream

332   consequence of innate immune signaling through the major nucleic-acid-sensing immune pathways.

333   Treatment with poly(I:C) did not recapitulate the acute toxicity induced by treatment with PS-modified

334   ASOs, suggesting that the PS-ASO-induced motor phenotypes do not result from TLR3- or MDA-5-

335   mediated effects. And experiments in Myd88^{-/-} STING^{-/-} mice confirmed that PS-ASO-induced motor

336   phenotypes are not mediated by TLR7, TLR9, or cGAS/STING.

337   At least part of the acute neurotoxicity of PS-ASOs is likely to be mediated by protein binding, for

338   example, to cell surface receptors involved in neuronal signaling. PS-DNA shows extensive binding to a

339   variety of proteins,[47-50] including cell-surface and trafficking proteins.[51-54] The origins of the high protein

340   binding of PS-oligos were recently explored with a structural study.[55] After systemic administration, an

341   earlier generation of mixed-backbone modification ASOs showed reduced binding to proteins such as

342   complement pathway members and clotting factors.[56-59] An explanation of the acute motor phenotypes

15

343   related to protein binding is also consistent with the sugar modification data presented above, since PS-

344   MOE reduces nonspecific protein binding relative to PS-DNA;[60] for example, recent work showed that

345   PS-MOE bound various plasma proteins with 3 to 50-fold lower affinity relative to PS-DNA.[61] In another

346   recent study, PS-2'OMe gapmers of two different sequences showed about 2.5-fold lower affinity

347   protein binding than PS-DNA of the same sequence.[55]

348   The acute motor phenotypes discussed in this work do not appear to be related to other types of ASO-

349   induce toxicity – such as liver toxicity or immune stimulation. For example, in ongoing work in our

350   group, we have come across sequences that are well-tolerated in terms of acute motor phenotypes, but

351   still exhibit liver toxicity, and vice versa. The timing of these effects is also very different: with acute

352   motor phenotypes strongest in the first hour (perhaps driven by binding to cell-surface receptors as

353   discussed above), innate immune stimulation peaking at 1-2 days (driven by binding to toll-like receptors

354   and cytosolic nucleic acid sensors), and liver toxicity evident from 1 day to several days after dosing

355   (driven by factors including mislocalization of paraspeckle proteins to nucleoli[62]).

356   This paper has focused on a single mixed-backbone design, and the impact of replacing three PS linkages

357   within each MOE wing with their corresponding (unmodified) PO linkages. It is striking that a relatively

358   small reduction in PS content makes such a dramatic difference in acute toxicity for multiple sequences.

359   Our work on *C9ORF72* showed that this design not only maintained but improved potency relative to the

360   full PS version.[21] Other investigators have also disclosed that some ASOs show increased potency when

361   a subset of PS linkages are replaced by PO linkages.[63] Nevertheless, this design sometimes leads to a

362   modest loss in potency, as shown in Figure 4.

363   The well-tolerated nature of <u>fully 2'-modified</u> ASOs in the CNS (Figure 2) has allowed the rapid

364   development and FDA approval of nusinersen[5-9] as well as the first personalized ASO drug, milasen.[64]

365   However, recruitment of RNase H requires the presence either of DNA or a DNA analogue, typically as a

366   gapmer design.[65, 66] The fact that PS-DNA shows higher acute toxicity than the corresponding 2'-

367   modified nucleotides (Figure 2) suggests that a major area of focus for nucleic acid chemists should be

368   the development of sugar or phosphate-modified DNA analogues that elicit robust RNase H cleavage

369   while reducing the incidence of motor phenotypes when administered to the CNS. The development of

370   next-generation mixed-backbone ASOs is an active area of research in our group.[33, 67] In the meantime,

371   researchers can implement mixed backbone designs such as those described here, along with calcium

372   formulation, to improve the therapeutic index of gapmer ASOs for clinical use in the CNS.

373

16

374   **METHODS**

375   **Oligonucleotides**

376   All oligonucleotides were synthesized using ABI 394 or Akta OligoPilot synthesizers using standard

377   methods. Phosphoramidites were purchased from ChemGenes and diluted to 0.1 M in acetonitrile.

378   Sulfurization was accomplished using DDTT (0.1M, ChemGenes). Benzylthiotetrazole (0.25 M in

379   acetonitrile, TEDIA) was used as activator. All cytosine residues were 5-methylcytosine.

380   Oligonucleotides were deprotected by treatment with concentrated aqueous ammonia at 55°C for 16h

381   then concentrated and purified by ion-exchange HPLC (eluting with 30% acetonitrile in water containing

382   increasing gradients of $NaClO_4$) or ion-pairing reverse-phase HPLC (eluting with aqueous

383   triethylammonium acetate containing increasing gradients of acetonitrile). All oligonucleotides were

384   characterized by LCMS.

385   After HPLC purification, we carried out final desalting and buffer equilibration using ultrafiltration

386   (Amicon centrifugal filters, 3-kDa molecular weight cutoff, Millipore). For oligonucleotides administered

387   in PBS, we placed the oligonucleotide in the Amicon filter and washed with 2 changes of PBS. To

388   saturate calcium-binding sites within oligonucleotides, we placed the purified oligonucleotides in the

389   Amicon filter, washed them twice with a 20 mM solution of $CaCl_2$, twice with water, and once with PBS,

390   before resuspending the ASOs in PBS (Note, in follow up work after the completion of this study, we

391   found that a lower concentration of $CaCl_2$ was preferable to minimize compound loss during this wash

392   step, which is an issue for certain sequences). For the oligonucleotides used for sheep studies, we did

393   not carry out calcium saturation in this manner but rather resuspended in USP-grade Lactated Ringers

394   Solution (LRS, which contains 1.3 mM Ca^{2+}).

395

396   **ICV administration of oligonucleotides in mice**

397   Mouse studies were carried out under UMass Medical School IACUC protocol A-2551. FVB/NCI mice (7-

398   13 weeks old) were anaesthetized by intraperitoneal injection of fentanyl/midazolam/dexmedetomidine

399   (0.1, 5, and 0.25 mg/kg, respectively, as a solution in sterile saline). Anaesthetized animals were

400   transferred to a Kopf small animal stereotaxic frame, ear bars placed and a hand-warmer was placed

401   underneath the animal to preserve core body-temperature. Ophthalmic lubricant was placed over each

402   eye and the fur covering the skull was removed. The scalp was aseptically prepared by thorough

17

403   alternate swabbing with betadine and 70% isopropanol (3x each) and allowed to dry before a medial

404   incision was made to expose the skull. The periosteum was dried with a sterile cotton swab and the

405   syringe containing oligonucleotide was moved to bregma. A point was marked on the skull 1 mm

406   dextrolateral and 0.4 mm posterior from bregma and a 0.6–0.8-mm diameter hole drilled at this

407   location. The tip of the needle was advanced 2 mm ventrally through this hole into the lateral ventricle

408   and after a 2 minute wait, the oligonucleotide was injected over a period of 25 seconds (10 μL total

409   injection volume). The needle was left in place for 3 minutes post-injection, then removed and the skin

410   closed with 5-0 vicryl suture. An intraperitoneal injection of fluemazenil/atipamezole (0.5 mg/kg and 5

411   mg/kg respectively, in sterile saline) was used to reverse injected anesthetic agents. Buprenorphine was

412   also injected for analgesia (0.3 mg/kg, SC). Animals were removed from the stereotaxic frame and

413   allowed to recover in a warm cage, food and gel were provided, and the animals were observed

414   periodically over the next 24 hours according to the rubric laid out in Table 1.

415   For ICV injections in the Myd88^{-/-} STING^{-/-} mice (C57BL/6 background) and corresponding C57BL/6

416   controls, we used the protocol described above with slightly adjusted coordinates for the ICV injection

417   (1mm dextrolateral, 2mm posterior, 3mm ventral.)

418

419   **STING/MyD88 double knockout mice**

420   Myd88^{-/-} mice on C57BL/6 background[68] were obtained from S. Akira (Osaka University, Osaka, Japan).

421   STING^{-/-} mice on C57BL/6 background[69] were originally from G. Barber (University of Miami, Florida) and

422   obtained from D. Stetson (University of Washington, Seattle). The two strains were intercrossed to

423   generate Myd88^{-/-} STING^{-/-} double knockouts. The mice were bred and maintained under pathogen–free

424   conditions in our animal facility. The Myd88 and STING deficiencies were confirmed by performing PCR

425   on DNA obtained after digesting a tail snip. For Myd88, specific primer pairs were used to distinguish the

426   WT or knockout allele in two separate reactions. Reaction 1 with primer sequences AGC CTC TAC ACC

427   CTT CTC TTC TCC ACA and AGA CAG GCT GAG TGC AAA CTT GTG CTG was used to detect the WT band at

428   1000 bp and reaction 2 with primer pairs AGC CTC TAC ACC CTT CTC TTC TCC ACA and ATC GCC TTC TAT

429   CGC CTT CTT GAC GAG were used to detect KO band at 1000 bp. For STING, reaction 1 with primer

430   sequences AGA ACG GAC AGC CAG TAA GTA TAC AG and CAA TGC TCT CAT AGC CTT CAC TAT C was

431   used to detect the WT band at 375 bp and reaction 2 with primer pairs AAC TTC CTG ACT AGG GGA GGA

432   GTA G and CAA TGC TCT CAT AGC CTT CAC TAT C was used to detect the KO band at 470 base pairs.

433

18

ASO administration in sheep

Sheep studies were carried out under UMass Medical School IACUC protocol A-2593. Jacob sheep were fasted overnight in preparation for surgery. A 20G catheter was placed and secured in the jugular vein, blood (5 mL) was drawn from the catheter for analysis, and the catheter was flushed with saline (0.9% NaCl).   We administered buprenorphine (0.01 mg/kg IM), acepromazine (0.05 mg/kg IM) and glycopyrrolate (0.01 mg/kg IM) 30 min prior to induction of anesthesia. An intravenous cocktail of ketamine (6 mg/kg) and diazepam (0.3 mg/kg) was administered to induce anesthesia, followed by ketoprofen (2.2. mg/kg SQ) as analgesic and cefazolin (22 mg/kg IV) to minimizes any risk of infection. The animal was intubated, and a stomach tube was placed to prevent rumen gas pressure build up. Anesthesia was maintained using vaporized isoflurane (1.5–3.5% in oxygen). Sheep were positioned in lateral recumbency in an Allura Xper FD20 X-ray system (Philips Medical Systems, Best, Netherlands). A 19-gauge Tuohy needle was inserted in the lumbosacral (L7-S1) intrathecal space and then ~5 mL of CSF was removed. Using the Touhy needle as entry point, a straight tip microcatheter (Excelsior SL-10; Stryker Neurovascular) was inserted through the lumen of the needle to access the intrathecal space. The microcatheter was navigated into the cisterna magna with an assistance of a 0.014" wire under fluoroscopic guidance. The wire had a slight curve on the tip (Synchro Guidewire, Stryker Neurovascular) to avoid any nerve or vascular structure damage. A microcatheter contrast injection (1 mL of Omnipaque 240 mgI/ml) was injected and the pattern of contrast material distribution was visualized prior to the injection of ASO solution (2 mg/kg in ~3 mL of Lactated Ringers Solution; for comparison, the mouse doses of 15-35 nmol/mouse equate to about 4-10 mg/kg). Cone beam computed tomography (Allura Xper FD20 X-ray system) imaging was performed to confirm the final microcatheter position in the cisterna magna in relation to the nerve and vascular structures. At the end of the procedure the Touhy needle was withdrawn and the microcatheter was removed.

EvADINT scoring system for acute neurotoxicity

After ICV administration of ASOs to mice, a blinded investigator ranked the behavior of mice at multiple timepoints using the rubric laid out in Table 1. If a mouse died within the first 24 hours, its score was assigned to be 75; otherwise it was the sum of all other scores. Seizures, if observed, were scored based on severity; hyperactive or spastic behavior was also scored based on severity and included twitching, uncontrolled movement such as "popcorning" and other atypical motor phenotypes. Besides these elements, the score was based on the time elapsed until mice resumed normal posture and behavior;

19

465   for example, if a mouse required more than 1 hour but less than 2 hours to be able to right itself

466   (resume and maintain sternal posture) it would be given a score of 8.   Each mouse was individually

467   scored. Examples of scoring, with corresponding videos, are provided in Supporting Table S1. The

468   breakdown of scoring for each mouse is provided in Supporting Tables S2-S7.

469

470   **Evaluation of gene silencing in the CNS**

471   *For comparison of backbones on gene silencing efficacy:* Mice were euthanized at 3 weeks post-

472   treatment by cervical dislocation and the brain was immediately removed into ice-cold PBS. The brain

473   was placed in a brain matrix (Braintree scientific) and the most rostral 3 mm discarded. A 1-mm slice was

474   then taken and each side homogenized independently. The tissue was suspended in Affymetrix

475   homogenizing solution containing proteinase K and mechanically dissociated using a Quiagen Tissuelyser

476   with a 2mm tungsten carbide bead. The tubes were then incubated in a water bath at 65 °C until all

477   tubes appeared transparent. Tubes were centrifuged (16,000 xG, 15 minutes) and supernatant

478   transferred to a 96 well plate for storage at -80.   *Htt, Malat1* and *Ppib* RNA levels were quantified using

479   the QuantiGene 2.0 assay kit (Affymetrix, QS0011) as previously described.[70]

480   *For studying the effect calcium formulation on gene silencing efficacy:* Mice were euthanized at 2 weeks

481   post-injection via IP administration of 0.1mL of 390 mg/mL pentobarbital sodium and the brain and

482   spinal cord were immediately removed into ice-cold PBS. A 2mm section of the lumbar spinal cord was

483   cut and placed in an Eppendorf tube in -80°C. The brain was placed in a brain matrix and the most

484   rostral 3mm discarded. A 2-mm slice was taken, and the cortical section removed and placed in an

485   Eppendorf tube in -80°C. Tissue was homogenized in TRI-reagent using a Qiagen TissueLyser and 1 μg of

486   RNA was reverse transcribed using High-Capacity cDNA Reverse Transcription kit (Life Technologies) per

487   the manufacturer's protocol. qRT-PCR was carried out using iTaq Supermix (Bio-Rad) on Bio-Rad CFX-96

488   real time machine using gene-specific primers: *Malat1* Primer1: 5' CTC CAA CAA CCA CTA CTC CAA 3';

489   Primer2: 5' GTA CTG TTC CAA TCT GCT GCT A 3'; probe: /56-FAM/TCA TAC TCC /ZEN/AGT CGC GTC ACA

490   ATG C/3IABkFQ/. For *Ppib* (internal control), Primer1: 5'CCG TAG TGC TTC AGC TTG A 3'; Primer2: 5' AGC

491   AAG TTC CAT CGT GTC ATC 3'; Probe: /56-FAM/TGC TCT TTC /ZEN/CTC CTG TGC CAT CTC /3IABkFQ/.

492

493

20

494   **SUPPORTING INFORMATION / DATA AVAILABILITY**

495   Supporting information is available in the online version of this file, and includes the following:

496   Supporting Figure S1 shows the dose responsiveness of acute motor phenotypes. Supporting Table S1

497   and associated movies show examples of mouse phenotypes and corresponding assigned scores. Tables

498   S2-S10 provide a breakdown of the EvADINT scoring for each mouse and each treatment.

499

500   **ACKNOWLEDGEMENTS**

508

509   **AUTHOR CONTRIBUTIONS**

510   MPM and PMK synthesized and purified oligonucleotides; MPM, JMR-B, FW and AW carried out mouse

511   experiments; FW, JMR-B and JKW developed the EvADINT scoring assay; MPM, JMR-B, M.Marosfoi, RMK

512   and HG-E carried out the sheep study; M.Motwani and KAF developed the knockout mice, JKW

513   supervised the study and wrote the manuscript; all authors edited the manuscript.

514

515   **COMPETING INTERESTS**

516   JKW is Scientific Advisory Board member of PepGen and ad hoc consultant for BridgeBio and Flagship

517   Pioneering. RHB is co-founder and Scientific Advisory Board member of ApicBio.

518

519   **REFERENCES**

21

520   1.   Seguin, R., Antisense Oligonucleotides for Treatment of Neurological Diseases. In
521   *Oligonucleotide-Based Drugs and Therapeutics: Preclinical and Clinical Considerations for*
522   *Development*. (eds. N. Ferrari & R. Seguin) 389-409 (Wiley, Hoboken; 2018).
523   2.   Evers, M.M., Toonen, L.J. & van Roon-Mom, W.M. (2015). Antisense oligonucleotides in therapy
524   for neurodegenerative disorders. Adv Drug Deliv Rev *87*, 90-103.
525   3.   Wahlestedt, C. (1994). Antisense oligonucleotide strategies in neuropharmacology. Trends
526   Pharmacol. Sci. *15*, 42-46.
527   4.   Smith, R.A., Miller, T.M., Yamanaka, K., Monia, B.P., Condon, T.P., Hung, G., Lobsiger, C.S., Ward,
528   C.M., McAlonis-Downes, M., Wei, H. et al. (2006). Antisense oligonucleotide therapy for
529   neurodegenerative disease. J. Clin. Invest. *116*, 2290-2296.
530   5.   Aartsma-Rus, A. (2017). FDA Approval of Nusinersen for Spinal Muscular Atrophy Makes 2016
531   the Year of Splice Modulating Oligonucleotides. Nucleic Acid Ther *27*, 67-69.
532   6.   Corey, D.R. (2017). Nusinersen, an antisense oligonucleotide drug for spinal muscular atrophy.
533   Nat. Neurosci. *20*, 497-499.
534   7.   Hua, Y., Sahashi, K., Hung, G., Rigo, F., Passini, M.A., Bennett, C.F. & Krainer, A.R. (2010).
535   Antisense correction of SMN2 splicing in the CNS rescues necrosis in a type III SMA mouse
536   model. Genes Dev. *24*, 1634-1644.
537   8.   Passini, M.A., Bu, J., Richards, A.M., Kinnecom, C., Sardi, S.P., Stanek, L.M., Hua, Y., Rigo, F.,
538   Matson, J., Hung, G. et al. (2011). Antisense Oligonucleotides Delivered to the Mouse CNS
539   Ameliorate Symptoms of Severe Spinal Muscular Atrophy. Sci. Trans. Med. *3*, 72ra18-72ra18.
540   9.   Rigo, F., Hua, Y., Krainer, A.R. & Bennett, C.F. (2012). Antisense-based therapy for the treatment
541   of spinal muscular atrophy. J. Cell Biol. *199*, 21-25.
542   10. Singh, N.N., Howell, M.D., Androphy, E.J. & Singh, R.N. (2017). How the discovery of ISS-N1 led
543   to the first medical therapy for spinal muscular atrophy. Gene Ther. *24*, 520-526.
544   11. Finkel, R.S., Mercuri, E., Darras, B.T., Connolly, A.M., Kuntz, N.L., Kirschner, J., Chiriboga, C.A.,
545   Saito, K., Servais, L., Tizzano, E. et al. (2017). Nusinersen versus Sham Control in Infantile-Onset
546   Spinal Muscular Atrophy. N. Engl. J. Med. *377*, 1723-1732.
547   12. Mercuri, E., Darras, B.T., Chiriboga, C.A., Day, J.W., Campbell, C., Connolly, A.M., Iannaccone,
548   S.T., Kirschner, J., Kuntz, N.L., Saito, K. et al. (2018). Nusinersen versus Sham Control in Later-
549   Onset Spinal Muscular Atrophy. N. Engl. J. Med. *378*, 625-635.
550   13. Kordasiewicz, H.B., Stanek, L.M., Wancewicz, E.V., Mazur, C., McAlonis, M.M., Pytel, K.A.,
551   Artates, J.W., Weiss, A., Cheng, S.H., Shihabuddin, L.S. et al. (2012). Sustained therapeutic
552   reversal of Huntington's disease by transient repression of huntingtin synthesis. Neuron *74*,
553   1031-1044.
554   14. Tabrizi, S., Leavitt, B., Kordasiewicz, H., Czech, C., Swayze, E., Norris, D.A., Baumann, T., Gerlach,
555   I., Schobel, S., Smith, A. et al. (2018). Effects of IONIS-HTTRx in Patients with Early Huntington's
556   Disease, Results of the First HTT-Lowering Drug Trial (CT.002). Neurology *90*.
557   15. Tabrizi, S.J., Leavitt, B.R., Landwehrmeyer, G.B., Wild, E.J., Saft, C., Barker, R.A., Blair, N.F.,
558   Craufurd, D., Priller, J., Rickards, H. et al. (2019). Targeting Huntingtin Expression in Patients with
559   Huntington's Disease. N. Engl. J. Med. *380*, 2307-2316.
560   16. DeVos, S.L., Miller, R.L., Schoch, K.M., Holmes, B.B., Kebodeaux, C.S., Wegener, A.J., Chen, G.,
561   Shen, T., Tran, H., Nichols, B. et al. (2017). Tau reduction prevents neuronal loss and reverses
562   pathological tau deposition and seeding in mice with tauopathy. Sci. Trans. Med. *9*, eaag0481.
563   17. Zhao, H.T., John, N., Delic, V., Ikeda-Lee, K., Kim, A., Weihofen, A., Swayze, E.E., Kordasiewicz,
564   H.B., West, A.B. & Volpicelli-Daley, L.A. (2017). LRRK2 Antisense Oligonucleotides Ameliorate α-
565   Synuclein Inclusion Formation in a Parkinson's Disease Mouse Model. Mol. Ther. Nucl. Acids *8*,
566   508-519.

567 18. Jiang, J., Zhu, Q., Gendron, Tania F., Saberi, S., McAlonis-Downes, M., Seelman, A., Stauffer,
568   Jennifer E., Jafar-nejad, P., Drenner, K., Schulte, D. et al. (2016). Gain of Toxicity from ALS/FTD-
569   Linked Repeat Expansions in *C9ORF72* Is Alleviated by Antisense Oligonucleotides Targeting
570   GGGGCC-Containing RNAs. Neuron *90*, 535-550.

571 19. Becker, L.A., Huang, B., Bieri, G., Ma, R., Knowles, D.A., Jafar-Nejad, P., Messing, J., Kim, H.J.,
572   Soriano, A., Auburger, G. et al. (2017). Therapeutic reduction of ataxin-2 extends lifespan and
573   reduces pathology in TDP-43 mice. Nature *544*, 367.

574 20. McCampbell, A., Cole, T., Wegener, A.J., Tomassy, G.S., Setnicka, A., Farley, B.J., Schoch, K.M.,
575   Hoye, M.L., Shabsovich, M., Sun, L. et al. (2018). Antisense oligonucleotides extend survival and
576   reverse decrement in muscle response in ALS models. J. Clin. Invest. *128*, 3558-3567.

577 21. Tran, H., Moazami, M.P., Yang, H., McKenna-Yasek, D., Douthwright, C., Pinto, C., Metterville, J.,
578   Shin, M., Sanil, N., Dooley, C. et al. (2021). Potent mixed backbone antisense oligonucleotide
579   safely suppresses expression of mutant c9orf72 transcripts and polydipeptides: First in human
580   pilot study. Research Square (preprint) *DOI: 10.21203/rs.3.rs-211236/v1*.

581 22. Khvorova, A. & Watts, J.K. (2017). The chemical evolution of oligonucleotide therapies of clinical
582   utility. Nature Biotechnology *35*, 238-248.

583 23. Watts, J.K., The medicinal chemistry of antisense oligonucleotides. In *Oligonucleotide-Based
584   Drugs and Therapeutics*. (eds. N. Ferrari & R. Seguin) 39-90 (Wiley, Hoboken; 2018).

585 24. Wan, W.B. & Seth, P.P. (2016). The medicinal chemistry of therapeutic oligonucleotides. J. Med.
586   Chem. *59*, 9645-9667.

587 25. Moser, V.C. (2011). Functional Assays for Neurotoxicity Testing. Toxicol. Pathol. *39*, 36-45.

588 26. OECD GUIDELINE FOR THE TESTING OF CHEMICALS (1997). Test No. 424: Neurotoxicity Study in
589   Rodents DOI 10.1787/20745788.

590 27. Murphy, V.A., Smith, Q.R. & Rapoport, S.I. (1986). Homeostasis of brain and cerebrospinal fluid
591   calcium concentrations during chronic hypo- and hypercalcemia. J. Neurochem. *47*, 1735-1741.

592 28. In more recent unpublished work, we have identified that 5 mM calcium is a better
593   concentration for this saturation protocol, since for some sequences 20 mM calcium leads to
594   reduced solubility.

595 29. Town, T., Jeng, D., Alexopoulou, L., Tan, J. & Flavell, R.A. (2006). Microglia Recognize Double-
596   Stranded RNA via TLR3. The Journal of Immunology *176*, 3804-3812.

597 30. Jiang, M., Zhang, S., Yang, Z., Lin, H., Zhu, J., Liu, L., Wang, W., Liu, S., Liu, W., Ma, Y. et al. (2018).
598   Self-Recognition of an Inducible Host lncRNA by RIG-I Feedback Restricts Innate Immune
599   Response. Cell *173*, 906-919.e913.

600 31. Kato, H., Takeuchi, O., Sato, S., Yoneyama, M., Yamamoto, M., Matsui, K., Uematsu, S., Jung, A.,
601   Kawai, T., Ishii, K.J. et al. (2006). Differential roles of MDA5 and RIG-I helicases in the recognition
602   of RNA viruses. Nature *441*, 101-105.

603 32. Toonen, L.J.A., Casaca-Carreira, J., Pellise-Tintore, M., Mei, H., Temel, Y., Jahanshahi, A. & van
604   Roon-Mom, W.M.C. (2018). Intracerebroventricular Administration of a 2'-O-Methyl
605   Phosphorothioate Antisense Oligonucleotide Results in Activation of the Innate Immune System
606   in Mouse Brain. Nucleic Acid Ther *28*, 63-73.

607 33. Debacker, A.J., Sharma, V.K., Meda Krishnamurthy, P., O'Reilly, D., Greenhill, R. & Watts, J.K.
608   (2019). Next-Generation Peptide Nucleic Acid Chimeras Exhibit High Affinity and Potent Gene
609   Silencing. Biochemistry *58*, 582-589.

610 34. Ostergaard, M.E., Southwell, A.L., Kordasiewicz, H., Watt, A.T., Skotte, N.H., Doty, C.N., Vaid, K.,
611   Villanueva, E.B., Swayze, E.E., Bennett, C.F. et al. (2013). Rational design of antisense
612   oligonucleotides targeting single nucleotide polymorphisms for potent and allele selective
613   suppression of mutant Huntingtin in the CNS. Nucleic Acids Res *41*, 9634-9650.

35. DeVos, S.L., Goncharoff, D.K., Chen, G., Kebodeaux, C.S., Yamada, K., Stewart, F.R., Schuler, D.R., Maloney, S.E., Wozniak, D.F., Rigo, F. et al. (2013). Antisense Reduction of Tau in Adult Mice Protects against Seizures. J. Neurosci. *33*, 12887-12897.

36. Meng, L., Ward, A.J., Chun, S., Bennett, C.F., Beaudet, A.L. & Rigo, F. (2014). Towards a therapy for Angelman syndrome by targeting a long non-coding RNA. Nature *518*, 409.

37. Friedrich, J., Kordasiewicz, H.B., O'Callaghan, B., Handler, H.P., Wagener, C., Duvick, L., Swayze, E.E., Rainwater, O., Hofstra, B., Benneyworth, M. et al. (2018). Antisense oligonucleotide-mediated ataxin-1 reduction prolongs survival in SCA1 mice and reveals disease-associated transcriptome profiles. JCI insight *3*, e123193.

38. Luo, X., Fitzsimmons, B., Mohan, A., Zhang, L., Terrando, N., Kordasiewicz, H. & Ji, R.-R. (2018). Intrathecal administration of antisense oligonucleotide against p38α but not p38β MAP kinase isoform reduces neuropathic and postoperative pain and TLR4-induced pain in male mice. Brain. Behav. Immun. *72*, 34-44.

39. Sztainberg, Y., Chen, H.M., Swann, J.W., Hao, S., Tang, B., Wu, Z., Tang, J., Wan, Y.W., Liu, Z., Rigo, F. & Zoghbi, H.Y. (2015). Reversal of phenotypes in MECP2 duplication mice using genetic rescue or antisense oligonucleotides. Nature *528*, 123-126.

40. Moore, L.R., Rajpal, G., Dillingham, I.T., Qutob, M., Blumenstein, K.G., Gattis, D., Hung, G., Kordasiewicz, H.B., Paulson, H.L. & McLoughlin, H.S. (2017). Evaluation of Antisense Oligonucleotides Targeting ATXN3 in SCA3 Mouse Models. Mol. Ther. Nucl. Acids *7*, 200-210.

41. Mohan, A., Fitzsimmons, B., Zhao, H.T., Jiang, Y., Mazur, C., Swayze, E.E. & Kordasiewicz, H.B. (2017). Antisense oligonucleotides selectively suppress target RNA in nociceptive neurons of the pain system and can ameliorate mechanical pain. Pain *159*, 139-149.

42. Ling, K.K., Jackson, M., Alkam, D., Liu, D., Allaire, N., Sun, C., Kiaei, M., McCampbell, A. & Rigo, F. (2018). Antisense-mediated reduction of EphA4 in the adult CNS does not improve the function of mice with amyotrophic lateral sclerosis. Neurobiol. Dis. *114*, 174-183.

43. Berridge, M.J. (1998). Neuronal Calcium Signaling. Neuron *21*, 13-26.

44. Brini, M., Cali, T., Ottolini, D. & Carafoli, E. (2014). Neuronal calcium signaling: function and dysfunction. Cell. Mol. Life Sci. *71*, 2787-2814.

45. Bosakowski, T. & Levin, A.A. (1987). Comparative acute toxicity of chlorocitrate and fluorocitrate in dogs. Toxicology and Applied Pharmacology *89*, 97-104.

46. Olson, R.E., Cacace, A.M., Hagedorn, P., Hog, A.M., Jensen, M.L., Nielsen, N.F., Li, D., Brown, J.M. & Mercer, S.E. (2016). Tau antisense oligomers and uses thereof. Patent application WO 2016/126995 A1.

47. Brown, D.A., Kang, S.H., Gryaznov, S.M., DeDionisio, L., Heidenreich, O., Sullivan, S., Xu, X. & Nerenberg, M.I. (1994). Effect of phosphorothioate modification of oligodeoxynucleotides on specific protein binding. Journal of Biological Chemistry *269*, 26801-26805.

48. Lebedeva, I. & Stein, C.A. (2001). Antisense oligonucleotides: promise and reality. Annual Review of Pharmacology and Toxicology *41*, 403-419.

49. Levin, A.A., Yu, R.Z. & Geary, R.S., Basic Principles of the Pharmacokinetics of Antisense Oligonucleotide Drugs. In *Antisense Drug Technology: Principles, Strategies, and Applications*, Edn. 2nd. (ed. S.T. Crooke) 183-215 (CRC Press, Boca Raton; 2008).

50. Geary, R.S. (2009). Antisense oligonucleotide pharmacokinetics and metabolism. Expert Opin Drug Met *5*, 381-391.

51. Weidner, D.A., Valdez, B.C., Henning, D., Greenberg, S. & Busch, H. (1995). Phosphorothioate oligonucleotides bind in a non sequence-specific manner to the nucleolar protein C23/nucleolin. FEBS Letters *366*, 146-150.

52. Stein, C.A., Wu, S., Voskresenskiy, A.M., Zhou, J.F., Shin, J., Miller, P., Souleimanian, N. & Benimetskaya, L. (2009). G3139, an anti-Bcl-2 antisense oligomer that binds heparin-binding

| | | growth factors and collagen I, alters in vitro endothelial cell growth and tubular morphogenesis. Clin. Cancer Res. *15*, 2797-2807. |

53. Miller, C.M., Donner, A.J., Blank, E.E., Egger, A.W., Kellar, B.M., Østergaard, M.E., Seth, P.P. & Harris, E.N. (2016). Stabilin-1 and Stabilin-2 are specific receptors for the cellular internalization of phosphorothioate-modified antisense oligonucleotides (ASOs) in the liver. Nucleic Acids Research *44*, 2782-2794.

54. Wang, S., Allen, N., Vickers, T.A., Revenko, A.S., Sun, H., Liang, X.H. & Crooke, S.T. (2018). Cellular uptake mediated by epidermal growth factor receptor facilitates the intracellular activity of phosphorothioate-modified antisense oligonucleotides. Nucleic Acids Res *46*, 3579-3594.

55. Hyjek-Skladanowska, M., Vickers, T.A., Napiorkowska, A., Anderson, B.A., Tanowitz, M., Crooke, S.T., Liang, X.H., Seth, P.P. & Nowotny, M. (2020). Origins of the Increased Affinity of Phosphorothioate-Modified Therapeutic Nucleic Acids for Proteins. J. Am. Chem. Soc. *142*, 7456-7468.

56. Agrawal, S., Rustagi, P.K. & Shaw, D.R. (1995). Novel enzymatic and immunological responses to oligonucleotides. Toxicology Letters *82-83*, 431-434.

57. Zhang, R., Iyer, R.P., Yu, D., Tan, W., Zhang, X., Lu, Z., Zhao, H. & Agrawal, S. (1996). Pharmacokinetics and tissue disposition of a chimeric oligodeoxynucleoside phosphorothioate in rats after intravenous administration. J. Pharmacol. Exp. Ther. *278*, 971-979.

58. Zhao, Q., Temsamani, J., Iadarola, P.L., Jiang, Z. & Agrawal, S. (1996). Effect of different chemically modified oligodeoxynucleotides on immune stimulation. Biochem. Pharmacol. *51*, 173-182.

59. Agrawal, S., Jiang, Z., Zhao, Q., Shaw, D., Sun, D. & Saxinger, C. (1997). Mixed-Backbone Oligonucleotides Containing Phosphorothioate and Methylphosphonate Linkages as Second Generation Antisense Oligonucleotide. Nucleosides Nucleotides *16*, 927-936.

60. Henry, S.P., Kim, T.-W., Kramer-Stickland, K., Zanardi, T.A., Fey, R.A. & Levin, A.A., Toxicologic Properties of 2'-O-Methoxyethyl Chimeric Antisense Inhibitors in Animals and Man. In *Antisense Drug Technology: Principles, Strategies and Applications.* (ed. S.T. Crooke) 327-363 (CRC Press, Boca Raton; 2007).

61. Gaus, H.J., Gupta, R., Chappell, A.E., Ostergaard, M.E., Swayze, E.E. & Seth, P.P. (2019). Characterization of the interactions of chemically-modified therapeutic nucleic acids with plasma proteins using a fluorescence polarization assay. Nucleic Acids Res *47*, 1110-1122.

62. Shen, W., De Hoyos, C.L., Migawa, M.T., Vickers, T.A., Sun, H., Low, A., Bell, T.A., 3rd, Rahdar, M., Mukhopadhyay, S., Hart, C.E. et al. (2019). Chemical modification of PS-ASO therapeutics reduces cellular protein-binding and improves the therapeutic index. Nat. Biotechnol. *37*, 640-650.

63. Ferrari, N. & Seguin, R. (2012). Oligonucleotide inhibitors with chimeric backbone and 2-amino-2'-deoxyadenosine. PCT application PCT/CA2012/000169.

64. Kim, J., Hu, C., Moufawad El Achkar, C., Black, L.E., Douville, J., Larson, A., Pendergast, M.K., Goldkind, S.F., Lee, E.A., Kuniholm, A. et al. (2019). Patient-Customized Oligonucleotide Therapy for a Rare Genetic Disease. N. Engl. J. Med. *381*, 1644-1652.

65. Damha, M.J., Wilds, C.J., Noronha, A., Brukner, I., Borkow, G., Arion, D. & Parniak, M.A. (1998). Hybrids of RNA and arabinonucleic acids (ANA and 2'F-ANA) are substrates of Ribonuclease H. J. Am. Chem. Soc. *120*, 12976-12977.

66. Verbeure, B., Lescrinier, E., Wang, J. & Herdewijn, P. (2001). RNase H mediated cleavage of RNA by cyclohexene nucleic acid (CeNA). Nucleic Acids Research *29*, 4941-4947.

708   67.   Sharma, V.K., Singh, S.K., Krishnamurthy, P.M., Alterman, J.F., Haraszti, R.A., Khvorova, A.,
709   Prasad, A.K. & Watts, J.K. (2017). Synthesis and biological properties of triazole-linked locked
710   nucleic acid. Chem. Commun. *53*, 8906-8909.
711   68.   Adachi, O., Kawai, T., Takeda, K., Matsumoto, M., Tsutsui, H., Sakagami, M., Nakanishi, K. &
712   Akira, S. (1998). Targeted disruption of the MyD88 gene results in loss of IL-1- and IL-18-
713   mediated function. Immunity *9*, 143-150.
714   69.   Ishikawa, H. & Barber, G.N. (2008). STING is an endoplasmic reticulum adaptor that facilitates
715   innate immune signalling. Nature *455*, 674-678.
716   70.   Coles, A.H., Osborn, M.F., Alterman, J.F., Turanov, A.A., Godinho, B.M., Kennington, L., Chase, K.,
717   Aronin, N. & Khvorova, A. (2016). A High-Throughput Method for Direct Detection of
718   Therapeutic Oligonucleotide-Induced Gene Silencing In Vivo. Nucleic Acid Ther *26*, 86-92.

719